

# Gas-Phase Infrared Spectrum of the Protonated Water Dimer

Knut R. Asmis,<sup>1\*</sup> Nicholas L. Pivonka,<sup>2,3</sup> Gabriele Santambrogio,<sup>1</sup> Mathias Brümmer,<sup>1</sup> Cristina Kaposta,<sup>1</sup> Daniel M. Neumark,<sup>2,3\*</sup> Ludger Wöste<sup>1</sup>

The protonated water dimer is a prototypical system for the study of proton transfer in aqueous solution. We report infrared photodissociation spectra of cooled  $\text{H}^+(\text{H}_2\text{O})_2$  [and  $\text{D}^+(\text{D}_2\text{O}_2)$ ] ions, measured between 620 and 1900 wave numbers ( $\text{cm}^{-1}$ ). The experiment directly probes the shared proton region of the potential energy surface and reveals three strong bands below  $1600 \text{ cm}^{-1}$  and one at  $1740 \text{ cm}^{-1}$  (for  $\text{H}_5\text{O}_2^+$ ). From a comparison to multidimensional quantum calculations, the three lower energy bands were assigned to stretching and bending fundamentals involving the  $\text{O}\cdots\text{H}^+\cdots\text{O}$  moiety, and the highest energy band was assigned to a terminal water bend. These results highlight the importance of intermode coupling in shared proton systems.

Proton transfer through hydrogen bonds plays an essential role in many chemical and biological processes. The dynamics of proton transfer across biomembranes, for example, governs the bioenergetic functions of protein assemblies like the adenosine triphosphate synthetase complex (1) and bacteriorhodopsin (2). The detailed molecular mechanisms of these “proton pumps” remain elusive (3, 4). The anomalously high proton mobility of liquid water (5) indicates that, unlike other ions, the transport of protons in aqueous solutions does not require the net diffusion of atomic (or molecular) species but instead involves chemical exchange of hydrogen nuclei along charge-conducting “water wires” in which the hydrated proton forms a fluxional defect in the hydrogen-bonded network (6–8). Important limiting structures in these networks are the hydrated hydronium and hydrated proton complexes  $\text{H}_3\text{O}^+(\text{H}_2\text{O})_3$  and  $\text{H}^+(\text{H}_2\text{O})_2$  (9).

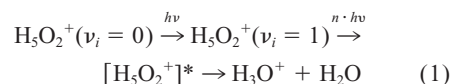
The interpretation of the spectroscopic signature of hydrated protons in liquid water, characterized by a quasi-continuous absorption observed in the infrared (IR), has been a long-running controversy (10), in particular the attribution of specific bands to the hydrated proton structures  $\text{H}_5\text{O}_2^+$  and  $\text{H}_9\text{O}_4^+$  (11, 12). Spectroscopic information on the corresponding isolated gas-phase cluster ions, which could aid in the assignment, remains scarce. The vibrational spectroscopy of  $\text{H}_5\text{O}_2^+$  has been studied in the region of the free O–H stretch modes ( $>3500 \text{ cm}^{-1}$ ) with the use of infrared multiphoton photodissociation (IRMPD) spectroscopy (13, 14). The

experiments support a “solution-like”  $\text{H}_2\text{O}\cdots\text{H}^+\cdots\text{OH}_2$  structure, in which the proton is located symmetrically between the two water ligands; electronic structure calculations (15, 16) confirm that this species has a minimum energy structure with  $\text{C}_2$  symmetry as shown in the inset of Fig. 1. However, the vibrational modes involving the central proton, which are key to the understanding of proton transfer on the  $\text{H}_5\text{O}_2^+$  potential energy surface, have remained experimentally unexplored.

Here, we describe an experimental study of the gas-phase vibrational spectroscopy of  $\text{H}_5\text{O}_2^+$  and its deuterated analog,  $\text{D}_5\text{O}_2^+$ , between 620 and  $1900 \text{ cm}^{-1}$ , the region of the  $\text{O}\cdots\text{H}^+\cdots\text{O}$  fundamentals. The experiments were performed with a novel tandem mass spectrometer–ion trap setup (17) in combination with radiation from the free electron laser for infrared experiments (FELIX) (18). These experiments draw on the pioneering work of Meijer and co-workers (19), who showed that FEL radiation is well suited to study the gas-phase vibrational spectroscopy of atomic and molecular clusters and cluster ions in the region below  $2000 \text{ cm}^{-1}$ . In particular, one can perform vibrational “action” spectroscopy of positive and negative ions in this frequency range (17, 20), in which absorption of IR light by mass-selected ions yields charged fragments that can be detected with nearly unit efficiency. Continuously tunable tabletop lasers do not have sufficient intensity below  $2000 \text{ cm}^{-1}$  for this type of experiment.

For the measurement of the IRMPD spectra, we formed a continuous beam of water-cluster cations in a Perkin Elmer SCIEX atmospheric ion spray source and transferred it through a  $60\text{-}\mu\text{m}$  orifice into a high vacuum chamber.  $\text{H}_5\text{O}_2^+$  cations were mass-selected and accumulated in a linear radio-frequency hexadecapole ion trap kept at a temperature

of  $\sim 100 \text{ K}$ . The ion trap was filled with helium buffer gas, which collisionally cooled the trapped cluster ions down to the ambient temperature within several microseconds. Cooling of the floppy  $\text{H}_5\text{O}_2^+$  ions before irradiation minimized the contribution of vibrational hot bands and energetically low-lying isomers to the spectra. The trapped ions were irradiated by a single FEL macropulse, for which the overall pulse energy and duration were 20 to 40 mJ and 5  $\mu\text{s}$ , respectively. The full width at half maximum bandwidth was  $\sim 0.5\%$  of the central frequency. The IR beam was focused through a 5-mm KBr window into the center of the ion trap with a 48-cm focal length KBr lens. The IRMPD spectrum was measured by mass-selectively monitoring the formation of  $\text{H}_3\text{O}^+$  as a function of FELIX wavelength.  $\text{H}_3\text{O}^+$  ions were formed by dissociation of  $\text{H}_5\text{O}_2^+$  subsequent to the absorption of multiple IR photons, as is shown in Eq. 1:



Here,  $h$  is Planck’s constant,  $v_i$  is the vibrational quantum number of the  $i$ th vibrational mode and  $n$  is the total number of absorbed photons. Although Eq. 1 is a multiphoton process, no production of  $\text{H}_3\text{O}^+$  occurs unless the first photon is resonant with a vibrational transition of the cold parent ion. In more detail (21–24), absorption of the first few photons occurs within the “discrete” regime, in which a particular vibrational mode of a molecule is excited resonantly. Higher excitation accesses the “quasi-continuum” regime in which the density of states is so high that the vibrational energy is rapidly randomized among all vibrational modes of the molecule. The transition between the two regimes depends on the vibrational density of states and the strengths of the interactions between vibrational modes. The cluster continues to absorb photons until it has enough energy to dissociate. The dissociation energy of  $\text{H}_5\text{O}_2^+$  is  $31.6 \text{ kcal/mol}$  (25), so 6 to 18 photons are needed for dissociation in the frequency range studied here.

The IRMPD spectrum of  $\text{H}_5\text{O}_2^+$  (Fig. 1A) comprises four bands of higher intensity (b to e) at 921, 1043, 1317, and  $1741 \text{ cm}^{-1}$  and an additional weaker feature at  $788 \text{ cm}^{-1}$  (a). The bands are more than 20 times wider ( $>100 \text{ cm}^{-1}$ ) than the laser bandwidth ( $\sim 5 \text{ cm}^{-1}$  at  $10 \mu\text{m}$ ). Additional fine structure is observed for bands b to e, with a spacing on the order of 30 (b and c) and  $\sim 70 \text{ cm}^{-1}$  (d), respectively (Table 1). In order to aid in the assignment of the bands, we recorded IRMPD spectra of  $\text{D}_5\text{O}_2^+$  (Fig. 1B). Four bands (b’ to e’), somewhat narrower, with less pronounced fine structure and with different relative intensities than in the  $\text{H}_5\text{O}_2^+$

<sup>1</sup>Institut für Experimentalphysik, Freie Universität Berlin, Arnimallee 14, D 14195 Berlin, Germany. <sup>2</sup>Department of Chemistry, University of California, <sup>3</sup>Chemical Sciences Division, Lawrence Berkeley National Laboratory, Berkeley, CA 94720, USA.

\*To whom correspondence should be addressed. E-mail: asmis@physik.fu-berlin.de (K.R.A.); dan@radon.cchem.berkeley.edu (D.M.N.)

## REPORTS

spectra, are observed. All four band maxima are red-shifted upon H-D substitution, with isotope shifts of 1.32 (b-b'), 1.31 (c-c'), 1.37 (d-d'), and 1.34 (e-e').

Previous theoretical studies have indicated that the IR spectrum of  $\text{H}_2\text{O}\cdots\text{H}^+\cdots\text{OH}_2$  is adequately described within the harmonic approximation only for those vibrational modes that predominantly involve the terminal water molecules (26, 27). These modes include the H-O-H rock, wag, and twist below  $600\text{ cm}^{-1}$ ; the H-O-H bend around  $1750\text{ cm}^{-1}$ ; and the O-H stretch above  $3600\text{ cm}^{-1}$ . Thus, we assigned band e at  $1741\text{ cm}^{-1}$  to the asymmetric bending motion of the water molecules in  $\text{H}_5\text{O}_2^+$ , calculated at  $1787\text{ cm}^{-1}$  at the B-CCD(T)/TZ2P (28) level of theory (16). We attribute the remaining bands (a to d) to modes involving the central  $\text{O}\cdots\text{H}^+\cdots\text{O}$  moiety, which include the symmetric and asymmetric stretch as well as two bending modes. The B-CCD(T)/TZ2P harmonic frequencies of these modes are 650, 794, 1505, and  $1596\text{ cm}^{-1}$  (16). Only the latter three transitions are dipole-allowed, and the asymmetric stretch ( $794\text{ cm}^{-1}$ ) has the largest calculated oscillator strength. The experimental spectrum reveals no

substantial signal in the region between  $1500$  and  $1650\text{ cm}^{-1}$  and only a weak band below  $850\text{ cm}^{-1}$ . Thus, we find no satisfactory agreement between the experimental spectrum and the calculated harmonic frequencies in the region between  $600$  and  $1600\text{ cm}^{-1}$ .

The failure of the harmonic picture for  $\text{H}_5\text{O}_2^+$  is not surprising, because the shared proton vibrates in a rather flat potential and will undergo large amplitude motion, similar to the bialide anions such as  $\text{BrHBr}^-$  that have been studied by a similar technique (20). Several calculations have been undertaken to correct for anharmonic effects in the IR spectrum of  $\text{H}_5\text{O}_2^+$  (26, 27, 29). Compared to the harmonic frequencies, these models (Table 2) predict that the asymmetric stretch is blue-shifted above  $1000\text{ cm}^{-1}$  and that the bend modes are red-shifted below  $1500\text{ cm}^{-1}$ , thus improving the overlap with the experimental spectrum. However, the various calculations disagree on the ordering and the relative intensities of the transitions. The most extensive calculations to date are the four-dimensional (4D) simulations of Sauer and co-workers (27), which account for coupling between all four modes involving the shared proton. At this level of theory, the asymmetric stretch is calculated at  $1158\text{ cm}^{-1}$ . The two bend fundamentals are red-shifted by roughly  $500\text{ cm}^{-1}$ , to  $968$  and  $1026\text{ cm}^{-1}$ , so that they lie below the asymmetric stretch. These three values compare rather favorably with the three experimental values of  $921$  (b),  $1043$  (c), and  $1317\text{ cm}^{-1}$  (d), in particular when the origin ( $1252\text{ cm}^{-1}$ ) and not the maximum of band d is considered.

The assignment suggested by this comparison is supported by the isotope shifts in the  $\text{D}_5\text{O}_2^+$  spectrum. The 4D simulations predict a 5% larger isotope shift for the

asymmetric stretch (H-D shift of 1.49) than for the bends (1.42 and 1.43). Experimentally (Table 1), we find a 4% larger shift between peaks d and d' than that for the other two sets of peaks, although our absolute values are somewhat smaller. Changes in the relative band intensities upon deuteration, in particular those of band e', can be attributed to the influence of combination bands involving the  $\text{O}\cdots\text{H}^+\cdots\text{O}$  modes. The 4D simulations predict strong combination bands in the  $1300$  to  $1450\text{ cm}^{-1}$  region of the  $\text{D}_5\text{O}_2^+$  spectrum. These could account for the strong increase of the relative intensity of band e' in the  $\text{D}_5\text{O}_2^+$  spectrum, nominally the terminal  $\text{D}_2\text{O}$  bend, as compared to that of band e in the  $\text{H}_5\text{O}_2^+$  spectrum. In  $\text{H}_5\text{O}_2^+$ , most of these combination bands are predicted above  $1950\text{ cm}^{-1}$ , i.e., outside our measurement window.

The origin of the finer structure in the  $\text{H}_5\text{O}_2^+$  spectrum is less clear. This species is a nearly prolate top with rotational constant  $A_c = 5.8\text{ cm}^{-1}$  (30). The  $30\text{-cm}^{-1}$  spacing in bands b and c is much larger than  $2A_c$  and thus cannot be from  $\Delta K = \pm 1$  rotational transitions associated with excitation of the bend vibrations. However, this spacing and the larger spacing in band d is probably too small to originate from combination bands involving the low-frequency torsional and/or wagging modes of the terminal water molecules; calculated (harmonic) values for the lowest frequency modes of this type range from  $120$  to  $240\text{ cm}^{-1}$  (15, 16, 29). A third possibility is that this structure originates from  $\Delta v = 0$  sequence bands involving at least one of these low-frequency modes. For this to be the case, there must be a substantial population of one to two excited levels of the mode in question,

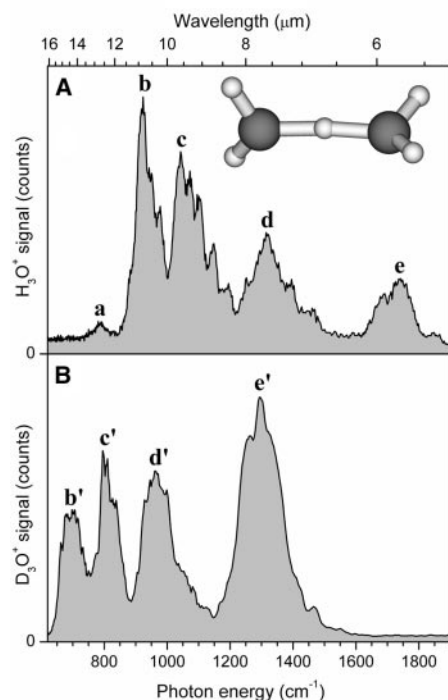


**Fig. 1.** IRMPD spectra of (A)  $\text{H}_5\text{O}_2^+$  and (B)  $\text{D}_5\text{O}_2^+$  in the spectral range from  $620$  to  $1900\text{ cm}^{-1}$ . Bands are labeled with lowercase letters. The shown traces are composite spectra, and the data was smoothed. The spectra were measured by monitoring the formation of  $\text{H}_3\text{O}^+$  ( $\text{D}_3\text{O}^+$ ) as a function of FELIX wavelength. The  $\text{H}_3\text{O}^+$  signal is superimposed over a small and wavelength-independent background resulting from collision-induced dissociation of the mass-selected  $\text{H}_5\text{O}_2^+$  ions with the He buffer gas atoms within the ion trap.

**Table 1.** Experimental vibrational frequencies [in wave numbers ( $\text{cm}^{-1}$ )] for  $\text{H}_5\text{O}_2^+$  and  $\text{D}_5\text{O}_2^+$  and isotope effects determined from IRMPD spectra. The position of each band maximum is underlined.

$\text{H}_5\text{O}_2^+$ band	Frequency	$\text{D}_5\text{O}_2^+$ band	Frequency	H-D shift
a	<u>788</u>			
b	<u>888</u> , <u>921</u> , 947, 975	b'	<u>697</u>	1.32
c	<u>1043</u> , 1071, 1100, 1145, 1195	c'	<u>795</u>	1.31
d	<u>1252</u> , <u>1317</u> , 1390, ~1460	d'	<u>960</u>	1.37
e	1687, <u>1741</u> , ~1850	e'	<u>1296</u>	1.34

**Table 2.** Comparison of experimental and calculated vibrational frequencies (in wave numbers) of the  $\text{O}\cdots\text{H}^+\cdots\text{O}$  moiety in  $\text{H}_5\text{O}_2^+$  (sym., symmetric; asym., asymmetric; x, out of plane; y, in plane). Tentative assignments based on the present study, frequencies from 4D simulation of Vener *et al.* (27), correlation-corrected vibrational self-consistent field frequencies (29), and harmonic frequencies at the B-CCD(T) level of theory (16) are listed.

Vibrational mode	Experiment	4D	CC-VSCF	Harmonic
$(\text{O}\cdots\text{H}\cdots\text{O})$ sym. stretch		587	599	650
$(\text{O}\cdots\text{H}\cdots\text{O})_x$ bend	921	968	1442	1505
$(\text{O}\cdots\text{H}\cdots\text{O})_y$ bend	1043	1026	1494	1596
$(\text{O}\cdots\text{H}\cdots\text{O})$ asym. stretch	1317	1158	1209	794

and its frequency must be  $30\text{ cm}^{-1}$  higher in the  $\nu = 1$  bend levels than in their ground states. A frequency shift of this type would be another example of the breakdown of the harmonic picture in  $\text{H}_5\text{O}_2^+$ .

In the 4D vibrational calculations, the asymmetric stretch was predicted to be more than three times more intense than the two bending bands in  $\text{H}_5\text{O}_2^+$ , which does not agree well with the experimental spectrum. This discrepancy can arise from at least two factors: (i) The calculations refer to the linear absorption spectrum, whereas the photoinduced vibrational predissociation mechanism (Eq. 1) governing our IRMPD experiments requires the absorption of multiple photons (6 to 18 photons in the frequency range studied). The absorption of the first few photons within the discrete (in contrast to quasi-continuum) regime (21, 22) generally governs the relative intensities observed in the IRMPD spectrum. Meijer and co-workers have found satisfactory agreement between the IRMPD and linear absorption spectrum for bi- and tricyclic hydrocarbon cations even though as many as 100 photons are required for dissociation (23, 24). However, these ions are larger than the protonated water dimer, and there may be more deviation from the linear absorption intensities over the spectral range probed by our experiment if more photons are needed to reach the quasi-continuum, a particular concern at the lowest frequencies in Fig. 1. (ii) Anharmonic coupling to vibrational modes other than the four  $\text{O}\cdots\text{H}^+\cdots\text{O}$  vibrations was not included in these calculations. The multiconfigurational self-consistent field calculations of Muguet (15) indicate that coupling to the water wags and bends is important. The fine structure in the experimental spectrum shows evidence for this type of coupling, which is likely to alter the overall intensity pattern.

The present results provide previously unstudied insight regarding the assignment of the liquid-phase spectra (12, 31). Hydrated protons in aqueous solution are characterized by four broad absorption bands at 1200, 1760, 2900, and  $3350\text{ cm}^{-1}$  and a continuous absorption over the 1000 to  $3400\text{ cm}^{-1}$  range. In heavy water, the spectral features are red-shifted to 920, 1420, 2130, and  $2480\text{ cm}^{-1}$ . On the basis of a comparison with the gas-phase spectra, the absorption of the hydrated proton (deuteron) in the 1200 and  $1760\text{ cm}^{-1}$  (920 and  $1420\text{ cm}^{-1}$ ) region can be attributed to the presence of  $\text{H}_5\text{O}_2^+$ -type structures in the aqueous solution. The bulk  $1760\text{ cm}^{-1}$  absorption is attributed to the blue-shifted bend vibration of the terminal water, which is found at  $1741\text{ cm}^{-1}$  in the present gas-phase spectrum. This result confirms the original assignment of Librovich *et al.* (11)

and recent multistate empirical valence-bond simulations by Kim *et al.* (12). The broad  $1200\text{ cm}^{-1}$  absorption is attributed to three modes, namely the asymmetric stretch and the two bend modes of the  $\text{O}\cdots\text{H}^+\cdots\text{O}$  moiety, that we find in the 920 to  $1320\text{ cm}^{-1}$  region. We note that the liquid-phase difference spectra also show a very weak absorption at around  $750\text{ cm}^{-1}$  and that a similar absorption is observed in our spectra at  $788\text{ cm}^{-1}$  (band a).

#### References and Notes

1. M. Saraste, *Science* **283**, 1488 (1999).
2. J. K. Lanyi, *J. Phys. Chem. B* **104**, 11441 (2000).
3. R. Pomès, B. Roux, *Biophys. J.* **82**, 2304 (2002).
4. A. M. Smondyrev, G. A. Voth, *Biophys. J.* **82**, 1460 (2002).
5. M. Eigen, L. D. Maeyer, *Proc. R. Soc. London* **247**, 505 (1958).
6. C. J. T. d. Grotthuss, *Ann. Chim. (Paris)* **58**, 54 (1806).
7. J. D. Lear, Z. R. Wasserman, W. F. DeGrado, *Science* **240**, 1177 (1988).
8. N. Agmon, *Chem. Phys. Lett.* **244**, 456 (1995).
9. D. Marx, M. E. Tuckerman, J. Hutter, M. Parinello, *Nature* **397**, 601 (1999).
10. G. Zundel, *Adv. Chem. Phys.* **111**, 1 (2000).
11. N. B. Librovich, V. P. Sakun, N. D. Sokolov, *Chem. Phys.* **39**, 351 (1979).
12. J. Kim, U. W. Schmitt, J. A. Gruetzmacher, G. A. Voth, N. E. Scherer, *J. Chem. Phys.* **116**, 737 (2002).
13. L. I. Yeh, J. D. Myers, J. M. Price, Y. T. Lee, *J. Chem. Phys.* **91**, 7319 (1989).
14. L. I. Yeh, Y. T. Lee, J. T. Hougen, *J. Mol. Spectrosc.* **164**, 473 (1994).
15. F. F. Muguet, *J. Mol. Struct.* **368**, 173 (1996).
16. E. D. Valeev, H. F. Schaefer III, *J. Chem. Phys.* **108**, 7197 (1998).
17. K. R. Asmris *et al.*, *Phys. Chem. Chem. Phys.* **4**, 1101 (2002).
18. G. M. H. Knippels, R. F. X. A. M. Mols, A. F. G. van der Meer, D. Oepts, P. W. van Amersfoort, *Phys. Rev. Lett.* **75**, 1755 (1995).
19. M. Putter, G. von Helden, G. Meijer, *Chem. Phys. Lett.* **258**, 118 (1996).
20. N. L. Pivonka *et al.*, *J. Chem. Phys.* **117**, 6493 (2002).
21. S. Mukamel, J. Jortner, *J. Chem. Phys.* **65**, 5204 (1976).
22. A. S. Sudbo, P. A. Schulz, E. R. Grant, Y. R. Shen, Y. T. Lee, *J. Chem. Phys.* **70**, 912 (1979).
23. J. Oomens, A. J. A. van Rooij, G. Meijer, G. von Helden, *Astrophys. J.* **542**, 404 (2000).
24. J. Oomens, G. Meijer, G. von Helden, *J. Phys. Chem. A* **105**, 8302 (2001).
25. Y. K. Lau, S. Ikuta, P. Kebarle, *J. Am. Chem. Soc.* **104**, 1462 (1982).
26. L. Ojamäe, I. Shavitt, S. J. Singer, *Int. J. Quantum Chem. Symp.* **29**, 657 (1995).
27. M. V. Vener, O. Kühn, J. Sauer, *J. Chem. Phys.* **114**, 240 (2001).
28. B-CCD(T) is the Brueckner coupled cluster doubles method with a perturbational triple-excitation correction. TZZP is the triple- $\zeta$  plus double polarization basis set.
29. G. M. Chaban, J. O. Jung, R. B. Gerber, *J. Phys. Chem. A* **104**, 2772 (2000).
30. D. J. Wales, *J. Chem. Phys.* **110**, 10403 (1999).
31. R. Vuilleumier, D. Borgis, *J. Chem. Phys.* **111**, 4251 (1999).
32. Supported by the Collaborative Research Center 546 and the Ph.D. Graduate Study Program 788 of the Deutsche Forschungsgemeinschaft. U.S. Air Force Office of Scientific Research grant F49620-00-1-0018 provided support for N.L.P. and D.M.N. We thank M. V. Vener and J. Sauer for helpful discussions, the Stichting voor Fundamenteel Onderzoek der Materie for providing the required beam time on FELIX, and the FELIX staff, in particular A. F. G. van der Meer, for skillful assistance.

18 December 2002; accepted 29 January 2003

Published online 4 January 2003;

10.1126/science.1081634

Include this information when citing this paper.

## Transformation of a Simple Plastic into a Superhydrophobic Surface

H. Yıldırım Erbil,<sup>1\*</sup> A. Levent Demirel,<sup>2\*</sup> Yonca Avcı,<sup>1</sup> Olcay Mert<sup>1</sup>

Superhydrophobic surfaces are generally made by controlling the surface chemistry and surface roughness of various expensive materials, which are then applied by means of complex time-consuming processes. We describe a simple and inexpensive method for forming a superhydrophobic coating using polypropylene (a simple polymer) and a suitable selection of solvents and temperature to control the surface roughness. The resulting gel-like porous coating has a water contact angle of  $160^\circ$ . The method can be applied to a variety of surfaces as long as the solvent mixture does not dissolve the underlying material.

Water repellency is important in many industrial and biological processes, such as the prevention of the adhesion of snow to antennas and windows, self-cleaning traffic indicators, the reduction of frictional drag on ship hulls, metal refining, stain-resistant textiles, and cell motility (1, 2). The hydrophobicity of a surface can be enhanced by a chemical modification that lowers the surface energy. This modification leads to an increase in the contact angle of a water drop, with a maxi-

imum value of approximately  $120^\circ$  reported for smooth  $\text{CF}_3$ -terminated surfaces (2–5). Superhydrophobic surfaces that have water contact angles larger than  $150^\circ$  have been obtained by controlling the surface topography of expensive hydrophobic materials by various processing methods, such as machining and etching (1–12). A superhydrophobic surface results from the increase of the surface roughness, so that the local geometry provides a large geometric area for a relative-